Prev. Nutr. Food Sci. 2023;28(3):360-369
https://doi.org/10.3746/pnf.2023.28.3.360
ISSN 2287-8602

Organoid Establishment of Long-Term Culture Using Primary Mouse Hepatocytes and Evaluation of Liver Function

Hye Mi Kim[1,2], Yerin Kim[1,3], Yuri Kim[1,2], Young Jun Kim[4], and Kwang Suk Ko[1,2]

[1]Department of Nutritional Science and Food Management and [2]Graduate Program in System Health Science and Engineering, Ewha Womans University, Seoul 03760, Korea
[3]Department of Medicine, Catholic Kwandong University College of Medicine, Gangwon 25601, Korea
[4]Department of Food and Biotechnology and Food and Regulatory Science, Korea University, Sejong 30019, Korea

ABSTRACT: Primary hepatocytes and various animal models have traditionally been used in liver function tests to assess the effects of nutrients. However, these approaches present several limitations such as time consumption, high cost, the need for facilities, and ethical issues in primary mouse hepatocytes and animal models. In this study, we constructed liver organoids from primary mouse hepatocytes (OrgPH) to replace primary hepatocytes and animal models. We isolated primary mouse hepatocytes from 6- to 10-week-old male C57BL/6J mice using the two-step collagenase method, and generated liver organoids by clustering the cells in Matrigel. To assess the hepatic function of OrgPH, we examined specific liver markers and gene expressions related to hepatic glucose, ethanol, and cholesterol metabolism. Over a 28-day culture period, liver-specific markers, including *Alb*, *Arg1*, *G6pc*, and *Cyp1a1*, increased or remained stable in the OrgPH. However, they eventually decreased in primary hepatocytes. Glucose and ethanol metabolism-related gene expression levels exhibited a similar tendency in AML12 cells and OrgPH. However, the expression levels of cholesterol metabolism-related genes displayed an opposite trend in OrgPH compared with those in AML12 cells. These results agree with those of previous studies involving *in vivo* models. In conclusion, our study indicates that OrgPH can retain liver function and mimic the hepatocytic physiology of mouse *in vivo* models. Therefore, organoids originating from primary mouse hepatocytes are potentially useful as an animal-free method for evaluating the safety and toxicity of health functional foods and a replacement for animal models.

Keywords: liver function, long-term culture, organoid, primary hepatocyte

INTRODUCTION

The liver plays an important role in metabolic homeostasis and numerous metabolic functions, including protein synthesis, hormone and bile production, and cholesterol and glucose homeostasis regulation (Builes Montaño et al., 2022; Chu et al., 2022; Liao et al., 2022). Liver cells consist of two major types: parenchymal and non-parenchymal cells. Parenchymal cells primarily comprise hepatocytes (~80%) and bile-duct epithelial cells (BECs, also known as cholangiocytes; ~20%), whereas non-parenchymal cells include Kupffer cells (macrophages), stellate cells, and sinusoidal endothelial cells (Jungermann and Kietzmann, 1996). BECs are responsible for bile acid collection and transportation, whereas hepatocytes are responsible for nutrient metabolism, xenobiotics, detoxification, and protein production (Miyajima et al., 2014; Rizki Safitri et al., 2018). Primary hepatocytes have proven to be useful tools in various biomedical studies, and have demonstrated their utility as *ex vivo* models for elucidating cellular and molecular events in liver physiology (Radko et al., 2019; Charni Natan and Goldstein, 2020). However, primary hepatocytes cannot be cultured for extended periods because this depletes liver function and viability under monolayer culture conditions (Sendi et al., 2018). Therefore, primary hepatocytes are unsuitable for long-term assay studies that require intact liver biology and specific functions (Bell et al., 2016). Ultimately, long-term culture methods for primary hepatocytes that can maintain liver metabolism and specific functions are necessary.

Health functional food ingredients must be evaluated for safety and functionality (Lee, 2013). The Organization for Economic Co-operation and Development (OECD)

Received 18 August 2023; Revised 31 August 2023; Accepted 31 August 2023; Published online 30 September 2023
Correspondence to Kwang Suk Ko, E-mail: kko@ewha.ac.kr

guidelines provide a standardized framework for conducting these evaluations (Kim et al., 2020b). The short-term dose toxicity evaluation results of single or multiple administration to animals within 24 h, according to OECD Test Guidelines (TG) 420, 423, and 425, and repeated dose toxicity evaluation results of administering health functional food ingredients to animals for 28 days or 90 days by long-term, according to OECD TG 408, 407, and 409, are to be submitted for safety and functionality for recognition (OECD, 2001; EFSA Scientific Committee, 2011; Jonsson et al., 2013). Additionally, the genotoxicity, reproductive toxicity, and chronic/carcinogenic toxicity results of animal tests must be submitted to confirm the safety and functionality of a health functional food. To comply with these OECD guidelines, a significant number of animals (at least 10 per group) must be used for each test, incurring significant costs and time constraints. Moreover, ethical concerns regarding animal testing have increased (MFDS, 2021a, 2021b). Accordingly, the requirement for experimental methods that replace animal experiments is increasing.

Cell lines and animal models have traditionally been used in several studies on the cellular signaling pathway, molecular development mechanism, and liver pathogenesis (Kim et al., 2020a). However, the two-dimensional (2D) culture of these cell lines is limited in terms of long-term and stable gene expression, while animal models are time consuming and expensive to develop (Milani Nejad and Janssen, 2014; Akbari et al., 2019). Organoids, which are three-dimensional (3D) cell culture systems, offer the structural and functional characteristics of an organ with self-renewal and maintained function (Kratochvil et al., 2019; Gómez Mariano et al., 2020). Organoids can mimic tissue structure and various cell types (Lancaster and Knoblich, 2014; Harrison et al., 2021). Several researchers have recently established organoids from adult tissues, such as the gut, brain, kidney, lung, retina, and liver (Qu et al., 2021). Because of their ability to replicate organ properties, organoids have been widely used in disease modeling, drug screening, and host-microbial interaction studies (Huch and Koo, 2015; Nakamura and Sato, 2017).

This study investigated the potential of liver organoids derived from primary mouse hepatocytes (OrgPH) to undergo long-term culture, mimic the functions of *in vivo* or *in vitro* environments, and serve as viable alternatives to animal models to ensure the safety and hepatic functional testing of health functional foods.

MATERIALS AND METHODS

Reagents for hepatocyte isolation

1X Hank's Balanced Salt solution (HBSS): 10X HBSS (Gibco), 1 M Hydroxyethyl piperazine ethane sulfonic acid (HEPES) buffer solution (Sigma-Aldrich Co.), and 7.5% $NaHCO_3$ (Daejung Chemical Co.); Solution 1: 1X HBSS, 34.2 mg/mL ethylene glycol-bis (2-aminoethyl ether) (Sigma-Aldrich Co.), and bovine serum albumin (BSA, RD tech); Solution 2: 1X HBSS, 0.4 M $CaCl_2-2H_2O$ (Junsei Chemical Co., Ltd.), and BSA; Collagenase solution: 1X HBSS, 1 mg/mL collagenase 1A (Sigma-Aldrich Co., C9891), and 0.4 M $CaCl_2-2H_2O$. All solutions were filtered using Steritop™ Filter Units (Millipore).

Isolation of primary mouse hepatocytes

Primary mouse hepatocytes were isolated from 6- to 10-weeks-old male C57BL/6J mice using two-step collagenase perfusion. Briefly, mice were anesthetized with isoflurane. Then, catheters were inserted the inferior vena cava, and the portal vein was immediately severed. Each mouse's liver was subsequently perfused with 50 mL of solution 1 (1X Hank's buffer) for 5 min. Next, the liver was digested with 50 mL of collagenase 1A solution (Sigma-Aldrich Co., C9891). The digested liver was subsequently extracted from the body and disrupted in a Petri dish until the liver lobes were dissociated into cells. After dissociation, the cells were filtered four times using a 70 μm filter (Corning) with solution 2. Subsequently, the filtered cells were centrifuged at 600 *g* for 3 min at 20°C. The Institutional Animal Care and Use Committee of Ewha Womans University approved all experimental animals (approval number: 21-018t).

Construction of organoids from primary mouse hepatocytes

Isolated primary mouse hepatocytes were enumerated and seeded at a concentration of 200 cells/μL in Matrigel (Corning) in a 24-well plate. The plate was subsequently incubated at 37°C for 40 min to allow Matrigel solidification. After Matrigel solidification, organoid media was added to the plate without disturbing the Matrigel dome. The organoid media comprised HepatiCultTM Organoid Growth Medium (STEMCELL Technologies), 1% (v/v) penicillin/streptomycin (Gibco), and 10 μM Y-27632 (Abmole BioScince) according to the manufacturer's instructions. The medium was replaced every 3～4 days, excluding the addition of Y-27632. OrgPH were passaged every 7～10 days.

AML12 cells and primary mouse hepatocyte cell culture

AML12 cells, which constitute a normal mouse hepatocyte cell line, were purchased from the American Type Culture Collection. AML12 cells were cultured in Dulbecco's Modified Eagle Medium/ F-12 (DMEN:F12; 1:1) medium (Hyclone™) supplemented with 10% fetal bovine serum (FBS) (Corning), 0.14 M sodium bicarbonate (Daejung), 1% penicillin and streptomycin (Gibco), 0.5 mM sodium pyruvate (Sigma-Aldrich Co.), and 40 ng/mL dexamethasone (Sigma-Aldrich Co.). The cells

were incubated at 37°C in a 5% CO_2 humidified incubator.

The primary mouse hepatocyte isolation procedure was the same as that described above. The isolated primary hepatocytes were cultured in DMEM:F12 (1:1) medium, FBS, 1% penicillin and streptomycin, 1 mM L-methionine (Sigma-Aldrich Co.), 7.5% sodium bicarbonate (Daejung), 1 mg/mL insulin, 0.1 mM hydrocortisone (Sigma-Aldrich Co.), and 1 M HEPES buffer solution (Sigma-Aldrich Co.). The cells were incubated at 37°C in a 5% CO_2 humidified incubator.

Determination of liver function in organoids from primary mouse hepatocytes

AML12 cells were seeded in a six-well plate at a density of 0.2×10^6 cells/well. After 4 h, AML12 cells were treated with 100 mM ethanol (Sigma-Aldrich Co.), 50 mM glucose (Sigma-Aldrich Co.), and 0.2 mg/mL cholesterol (Sigma-Aldrich Co.) for overnight.

OrgPH were embedded with Matrigel in a 48-well plate at a density of 200 cells/μL and the treatment concentrations of ethanol, glucose, and cholesterol were the same as those described above.

Real-time quantitative polymerase chain reaction

Total RNA was purified from OrgPH and primary hepatocytes using the AccuPrep® Universal RNA Extraction Kit (Bioneer) following the manufacturer's instructions. Total RNA from AML12 cells and liver tissue was purified using Trizol™ (Invtrogen™) following the manufacturer's instructions. cDNA was synthesized using the RevertAid First Strand cDNA Synthesis Kit (Thermo Fisher Scientific) following the manufacturer's instructions. Quantitative PCR (qPCR) was conducted based on the guidelines accompanying the Maxima SYBR Green/ROX qPCR Master Mix (Thermo Fisher Scientific). The relative expression levels of target mRNAs were normalized to glyceraldehyde 3-phosphate dehydrogenase (*Gapdh*), an internal control, using the $2^{-\Delta\Delta C_T}$ method (Livak and Schmittgen, 2001). All data are expressed as a relative quantity to each control value. The following primer sequences were used: albumin (*Alb*) forward and reverse primers: 5'-CCCTGATTACTCTGTATCCCT-3' and 5'-CCAAGTTCTTAGGCTCTTCTAC-3'; arginase 1 (*Arg1*) forward and reverse primers: 5'-CCCTAATGACAGCTCCTTTC-3' and 5'-CCACACTGACTCTTCCATTC-3'; glucose-6-phosphate (*G6pc*) forward and reverse primers: 5'-ATGACTTTGGGATCCAGTCG-3' and 5'-TGGAACCAGATGGGAAAGAG-3'; cytochrome P450 family 1 subfamily A (*Cyp1a1*) forward and reverse primers: 5'-GTCCAGCTGTCAGATGATAAGG-3' and 5'-TACATGAGGCTCCACGAGATA-3'; alcohol dehydrogenase (*Adh*) forward and reverse primers: 5'-GGGTGGACTTTTCGTTTGAA-3' and 5'-CTACGACGACGCTTACACCA-3'; acetaldehyde dehydrogenase (*Aldh*) forward and reverse primers: 5'-CTCGTACCTGGTGGATTTG-3' and 5'-CGTCGATGGGAATGGTTT-3'; cytochrome P450 2E1 (*Cyp2e1*) forward and reverse primers: 5'-AGTCTCTGGTTGACCCTAAG-3' and 5'-GGTCTCATGAACGAGGAATG-3'; glucose transporter 2 (*Glut2*) forward and reverse primers: 5'-CCCTTGTCACAGGCATTCTTA-3' and 5'-CACAGCAGATAGGCCAAGTAG-3'; glucokinase (*Gck*) forward and reverse primers: 5'-CATCAGGAGGCCAGTGTAAAG-3' and 5'-TCCCAGGTCTAAGGAGAGAAAG-3'; pyruvate kinase (*Pkm*) forward and reverse primers: 5'-TCCGGACTGGACTCATCAA-3' and 5'-GGATGTTCTCGTCACACTTCTC-3'; 3-hydroxy-3-methyl-glutaryl-CoA reductase (*Hmgcr*) forward and reverse primers: 5'-GACGAAGATGTGTCCAAGAG-3' and 5'-GAAGGCTAAACTCAGGGTAATC-3'; 3-hydroxy-3-methyl-glutaryl-CoA synthase (*Hmgcs*) forward and reverse primers: 5'-GATGGTGTAGATGCTGGAAAG-3' and 5'-CAGTCAGGCAAAGAGAGTTG-3'; sterol regulatory element-binding proteins 2 (*Srebp2*) forward and reverse primers: 5'-GGCGGACAACACACAATA-3' and 5'-GCCAGACTTGTGCATCTT-3'; *Gapdh* forward and reverse primers: 5'-CATCACTGCCACCCAGAAGACTG-3' and 5'-ATGCCAGTGAGCTTCCCGTTCAG-3'.

Statistical analysis

Data were analyzed using GraphPad PRISM 10 (GraphPad Software). Statistically significant mean differences in experimental liver-specific markers were analyzed using one-way analysis of variance (ANOVA) and post-hoc Tukey's and Dunnett's tests. Differences in liver functional enzyme activity between the two-groups were analyzed using the *t*-test. Statistical significance (*P*-value) was verified within 5%.

RESULTS

Morphological features of organoids from primary mouse hepatocytes

When hepatocytes were isolated from mouse liver and embedded in Matrigel, a single cell shape was observed. However, after 2~3 days, this shape changed to a cluster-like or hollow shape and eventually grew in size. Organoids were embedded in Matrigel and cultured for a week, followed by passaging one week later. Even after the culture, the same shape was observed during the first week of culture, and the same shape was observed even after repeated cultivation (Fig. 1).

Expression of liver-specific markers in organoids from primary mouse hepatocytes

Liver-specific markers, *Alb*, *Arg1*, *G6pc*, and *Cyp1a1* were selected to confirm the gene expression in OrgPH, AML12 cells, and primary mouse hepatocytes. The expression of

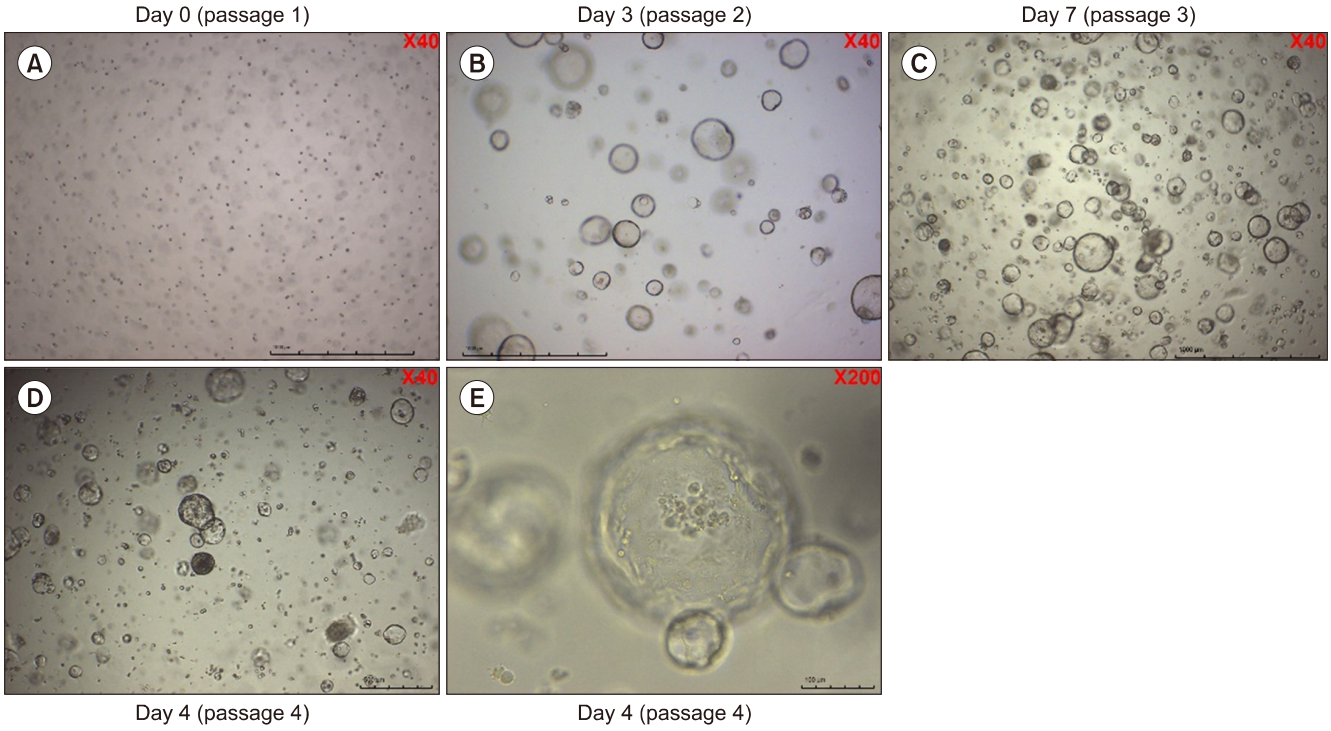

Fig. 1. Characterization of organoids from primary mouse hepatocytes. Organoids from primary mouse hepatocytes altered their morphology with time on day 0 at passage 1 (A), day 3 at passage 2 (B), day 7 at passage 3 (C), and day 4 at passage 4 (D and E) in Matrigel 3D culture after isolating primary hepatocytes from 7-week-old mice. Microscopic image of organoids with an original magnification of ×40 (A-D) and ×200 (E).

liver-specific marker genes, including *Alb* ($P<0.0001$), *Arg1* ($P<0.01$), *G6pc* ($P<0.001$), and *Cyp1a1* ($P<0.001$), in primary hepatocytes, was significantly higher than that in AML12 cells; nevertheless, the expression of these four markers eventually decreased in primary hepatocytes ($P<0.05$) (Fig. 2A).

Alb expression in OrgPH was significantly higher than that in AML12 cells on day 7 ($P<0.05$) but significantly lower on days 14 ($P<0.05$) and 28 ($P<0.01$). In contrast, the mRNA expression level of *Arg1* in OrgPH was confirmed to be elevated after 14 days, although no significant difference from the AML12 cells was noted on day 7. The expression level of *G6pc* in OrgPH was significantly higher than that in the AML 12 cells on day 7 ($P<0.05$), and it eventually increased. Finally, the expression level of *Cyp1a1* in OrgPH was consistent with that in AML12 cells on day 7; nonetheless, it eventually increased significantly ($P<0.05$) (Fig. 2B).

Assessment of glucose metabolism in organoids from primary mouse hepatocytes

Glucose treatment was administered to evaluate glucose metabolism in OrgPH. The mRNA expression levels of *Glut2* and *Pkm* increased significantly in the glucose-treated group compared with those in the control group ($P<0.05$, $P<0.01$) (AML12). However, the expression levels of *Glut2*, *Gck*, and *Pkm* genes in OrgPH were indifferent between the control and glucose-treated groups (Fig. 3).

Assessment of cholesterol metabolism in organoids from primary mouse hepatocytes

To evaluate cholesterol metabolism in OrgPH, both models were treated with cholesterol. The mRNA expression levels of the *Hmgcs*, *Hmgcr*, and *Srebp2* cholesterol metabolism-related genes decreased significantly in cholesterol-treated AML12 cells ($P<0.05$). However, the expression levels of *Hmgcs*, *Hmgcr*, and *Srebp2* genes in OrgPH increased significantly in the cholesterol-treated group compared with those in the control group ($P<0.01$, $P<0.05$). When treated with cholesterol, an opposite trend was observed in AML12 cells and OrgPH (Fig. 4).

Evaluation of ethanol metabolism in organoids from primary mouse hepatocytes

When AML12 cells were treated with ethanol, the mRNA expression levels of *Adh*, and *Aldh* increased significantly in the ethanol-treated group compared with those in the control group ($P<0.05$). However, *Cyp2e1* expression was increased compared with that in the control, although no statistical difference was confirmed. When OrgPH were treated with ethanol, *Adh*, *Aldh*, and *Cyp2e1* expression levels increased significantly in the ethanol-treated group compared with that in the control group ($P<0.05$) (Fig. 5).

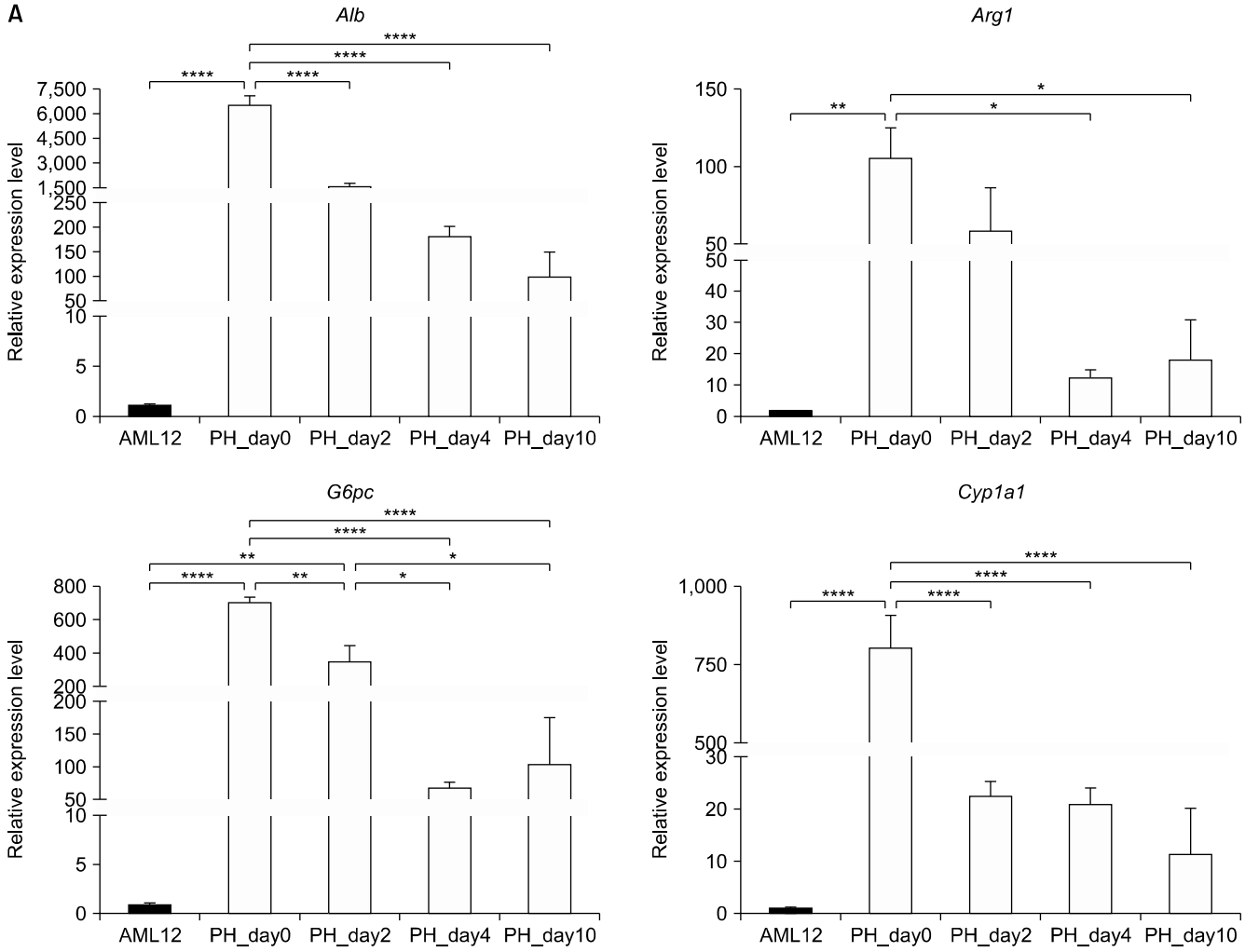

Fig. 2. mRNA expression levels of liver-specific markers in primary hepatocytes (A) and organoids from primary mouse hepatocytes compared with those in AML12 cells (B). *Alb*, *Arg1*, *G6pc*, and *Cyp1a1* were selected as liver-specific markers. Primary hepatocytes (PH) were cultured for 10 days after being isolated from mouse livers, and the expression levels of liver-specific markers were measured at 0, 2, 4, and 10 days using qPCR. OrgPH was cultured in Matrigel for 28 days after being isolated from mouse livers, and the expression level of liver-specific markers was measured at 7, 14, and 28 days using qPCR. All data are expressed as the mean±SD (n=3). Error bars represent the mean±SEM. *$P<0.05$, **$P<0.01$, and ****$P<0.0001$. PH, primary hepatocyte; OrgPH, liver organoids from primary mouse hepatocytes; G6Pc, glucose-6-phosphatase; CYP1A1, cytochrome P450 family 1 subfamily a member 1.

DISCUSSION

This study aimed to examine the capacity of OrgPH to achieve normal liver function and long-term culture. *In vivo* model experiments can be time consuming, and expensive and may raise ethical concerns because of animal use. Furthermore, for the safety and functionality of healthy functional foods to be recognized, numerous animals should be used because the results of single, repeated, genetic and chronic experiments must be submitted following the OECD guidelines (MFDS, 2021b). Alternative methods are required to replace or reduce the reliance on animal experiments. Additionally, *in vitro* models do not easily explain the functional and physiological changes of *in vivo* models (Kratochvil et al., 2019; Rezakhani et al., 2021). Therefore, this study focused on producing OrgPH using a 3D culture system. This approach enabled more effective simulation of an *in vivo* environment, providing a more physiologically relevant setting for studying liver function and responses. On comparing the results of OrgPH with those of AML12 cells, which are commonly used in normal mouse liver models, similar trends were observed.

Several studies have suggested that OrgPH morphology potentially exhibits a grape-like or hollow shape, whereas others have also suggested that it forms a rosette shape (Hu et al., 2018; Brooks et al., 2021; Nuciforo and Heim, 2020; Peng et al., 2021). In this study, a uniform shape was confirmed 2~3 days after embedding in Matrigel; the morphology assumed a grape-like shape after the first culture was initiated, and it gradually appearing hollow (Fig. 1).

To investigate the expression of common markers of liver metabolic function in OrgPH, we selected the major

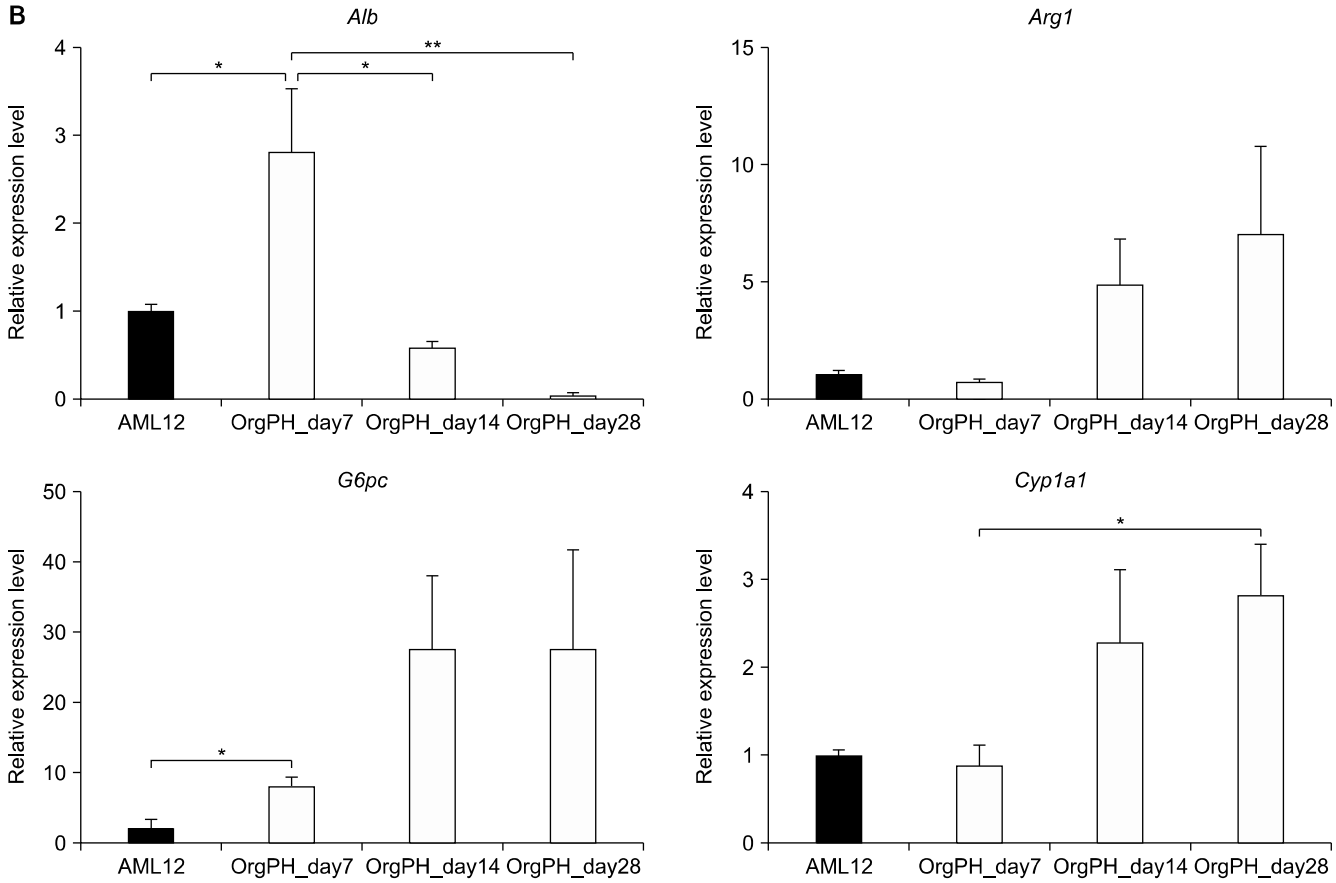

Fig. 2. Continued.

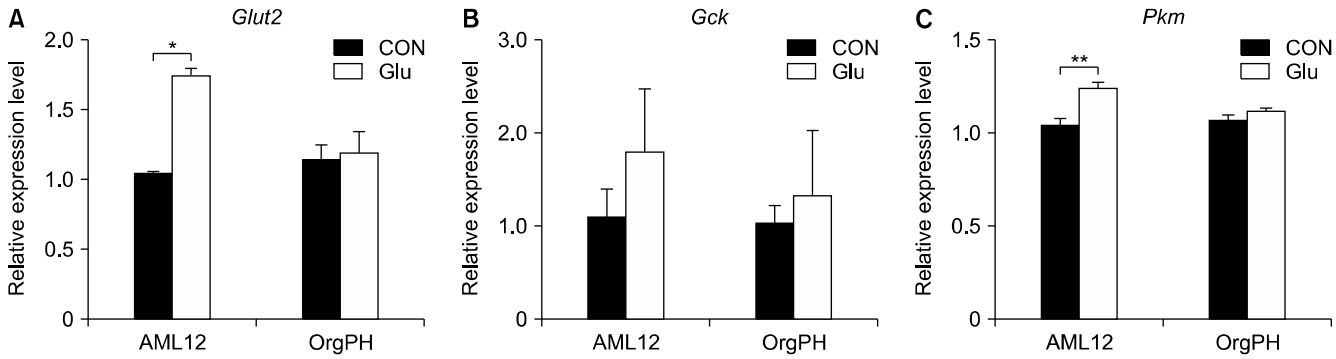

Fig. 3. mRNA expression levels of glucose metabolism genes in AML12 cells and organoids from primary mouse hepatocytes. AML12 cells and OrgPH were treated with 50-mM glucose for 24 h. The expression levels of *Glut2* (A), *Gck* (B), and *Pkm* (C) were determined using qPCR. All data are expressed as the mean±SD (n=3). Error bars represent the mean±SEM. $^{*}P<0.05$, and $^{**}P<0.01$ vs. control group. OrgPH, liver organoids from primary mouse hepatocytes; Glut2, glucose transport 2; GcK, glucokinase; PKM, pyruvate kinase.

liver metabolic markers related to the urea cycle, glucose homeostasis, and detoxification metabolism, including *Arg1*, *G6pc*, and *Cyp1a1*. Their expression levels were compared among AML12 cells, primary hepatocytes, and OrgPH (Zhu et al., 2020). The liver synthesizes albumin, which plays several roles, including the maintenance of osmotic pressure, the binding of various substances, such as hormones, drugs, and long-chain fatty acids, antioxidant activity, and anti-inflammatory functions (Miller and Jedrzejczak, 2001; Carvalho and Verdelho Machado, 2018). In primary hepatocytes, expression level of *Alb* peaked on day 0 after isolation from the liver, gradually decreasing with time. Furthermore, the expression levels of other genes, including *Arg1*, *G6pc*, and *Cyp1a1*, were significantly higher than those in AML12 cells on day 0; nevertheless, they gradually decreased over time (Fig. 2A). This could be because when primary hepatocytes are isolated from mouse liver tissue and cultured on a 2D monolayer, they experience a short life span and lack of cell proliferation, resulting in decreased metabolic function

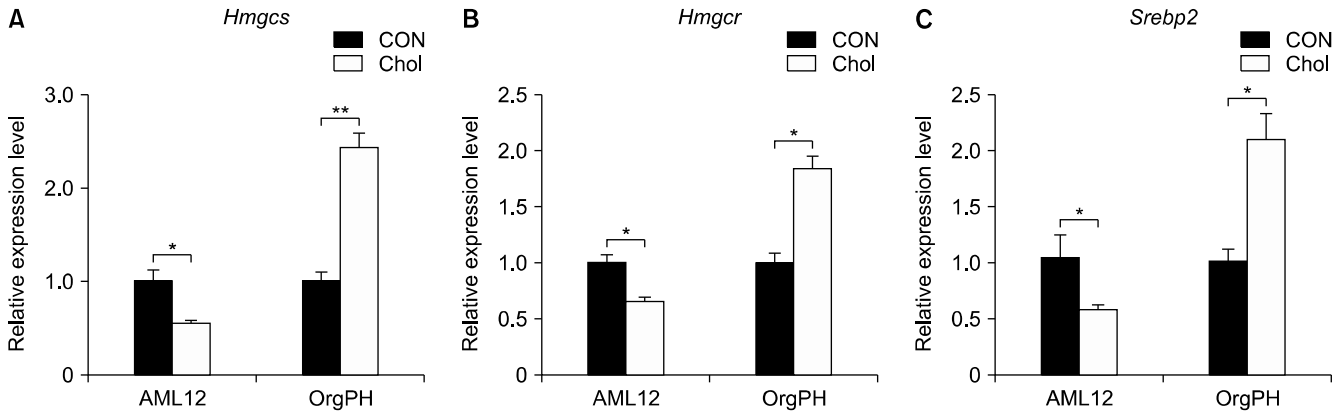

Fig. 4. mRNA expression levels of cholesterol metabolism-related genes in AML12 cells and organoids from primary mouse hepatocytes. AML12 cells and OrgPH were treated with 0.2 mg/mL cholesterol for 24 h. The expression levels of *Hmgcs* (A), *Hmgcr* (B), and *Srebp2* (C) were determined using qPCR. All data are expressed as the mean±SD (n=3). Error bars represent the mean±SEM. $^{*}P<0.05$, and $^{**}P<0.01$ vs. control group. OrgPH, liver organoids from primary mouse hepatocytes; HMGCS, 3-hydroxy-3-methyl-glutaryl-CoA synthase; HMGCR, 3-hydroxy-3-methyl-glutaryl-CoA reductase; SREBP2, sterol regulatory element-binding proteins 2.

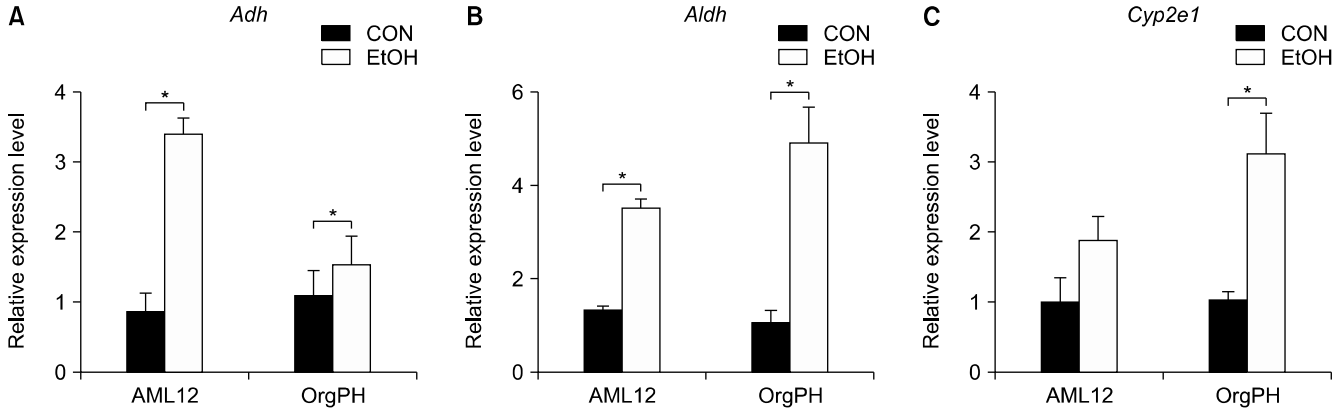

Fig. 5. mRNA expression levels of ethanol metabolism genes in AML12 cells and organoids from primary mouse hepatocytes. AML12 cells and OrgPH were treated with 100 mM ethanol for 24 h. The expression levels of *Adh* (A), *Aldh* (B), and *Cyp2e1* (C) were determined using qPCR. All data are expressed as the mean±SD (n=3). Error bars represent the mean±SEM. $^{*}P<0.05$ vs. control group. OrgPH, liver organoids from primary mouse hepatocytes; ADH, alcohol dehydrogenase; ALDH, aldehyde dehydrogenase 2; CYP2E1, cytochrome P450 2E1.

with time. Furthermore, primary hepatocytes rapidly lose their morphological characteristics (Shulman and Nahmias, 2012; Rose et al., 2021).

In contrast, *Arg1*, *G6pc*, and *Cyp1a1* expression levels in OrgPH gradually increased compared with those in AML12 cells (Fig. 2B). Thus, these results suggest that the OrgPH model is potentially more suitable for long-term experiments on the urea cycle, glucose homeostasis, and detoxification metabolism. However, the *Alb* expression level in OrgPH was lower than that in AML12 cells (Fig. 2B). Nevertheless, OrgPH maintained 50% of the *Alb* expression levels for 14 days. Therefore, these results suggest that OrgPH potentially performs liver metabolic functions and that the OrgPH model can mimic liver metabolic functions for a longer period than primary hepatocytes. Moreover, it can mitigate the difficulty of repeatedly isolating hepatocytes from mice for primary hepatocyte experimentation and circumvent ethical concerns.

To evaluate liver function in OrgPH, gene expression alterations confirmed upon treatment with ethanol, glucose, and cholesterol as well as the tendency of gene expression were compared with those in AML12 cells.

Ethanol is mandatorily eliminated from the body, and without its removal, it accumulates in the body, potentially causing various diseases and affecting metabolic pathways (Zakhari, 2006). Ethanol metabolism in the liver is initiated by ADH, ALDH, and CYP2E1 (Clemens, 2006). Eventually, ethanol is decomposed into water and carbon dioxide for easy elimination from the body (NIAAA, 2007). A previous study demonstrated decreased expression of *Adh* and *Aldh*, and increased expression of *Cyp2e1* in the livers of chronic ethanol-treated mice (Liu et al., 2012; Matson et al., 2013). Another study demonstrated an increased expression of *Aldh* in the livers of acute ethanol-treated mice (Bak et al., 2016). In our study, the expression levels of *Adh*, *Aldh*, and *Cyp2e1* increased

in OrgPH with acute and high-concentration ethanol (Katz et al., 2001; Liu et al., 2010), consistent with previous studies (Fig. 5). In summary, these results suggest that OrgPH potentially provides a hepatic *in vivo* environment for detoxification metabolism.

Glucose metabolism in the liver is an extremely important function in glycemic control. When blood glucose levels increase, the liver absorbs it via GLUT2 and is regulated by the rate-limiting enzymes GCK, G6Pc, and PKM (Han et al., 2016). In this study, glucose metabolism in OrgPH was evaluated and compared with that in AML12 cells. When AML12 cells were treated with glucose, *Glut2* and *Pkm* increased significantly; however, no significant difference was observed in OrgPH. However, the expression of corresponding genes was confirmed, suggesting that glucose metabolism can be evaluated using primary mouse hepatocyte-derived organoids.

Body cholesterol is synthesized in the liver via HMGCS, HMGCR, and SREBP2 gene regulation and potentially causes several health problems, including liver damage (Horton et al., 2002; Trapani et al., 2012; Liao et al., 2022). Therefore, we confirmed genetic changes based on cholesterol treatment. In AML 12 cells, the expression of the three genes decreased in the cholesterol-treated groups; nevertheless, opposite results were obtained in the cholesterol-treated groups of OrgPH (Fig. 4). In several studies on cholesterol diets in rodents, the expression of *Hmgcr*, *Hmgcs*, and *Srebp2* increased, and dietary cholesterol reportedly increased due to lipid metabolism disorders (Beppu et al., 2012; Chen et al., 2017; Liu et al., 2018). Interestingly, our data coincide with the experimental results from cholesterol diet-based liver function assessments using animal models, and these results suggest that OrgPH maintains a hepatic environment *in vivo*, even in long-term culture.

In conclusion, we examined the potential of OrgPH to maintain liver function during long-term culture. Liver function in primary hepatocytes decreased within two days after their isolation from the liver. However, it was maintained in OrgPH even during long-term culture, and hepatic functional metabolism was confirmed through glucose, ethanol, and cholesterol treatment. Therefore, OrgPH can be used to explain hepatic *in vivo* conditions and metabolism. Consequently, organoids can address the challenges encountered when using animal models and can be used in high-throughput drug screening and toxicity evaluation of health functional foods cheaply and with minimal use of animals. While further research is required to assess the efficiency of hepatocyte organoids in the hepatotoxicity evaluation of health functional foods, the organoid model is a potentially useful alternative to animal models.

FUNDING

This research was supported by the BK21 FOUR (Fostering Outstanding Universities for Research) funded by the Ministry of Education (MOE, Korea) and National Research Foundation of Korea (NRF-5199990614253, Education Research Center for 4IR-Based Health Care).

This research was supported by grants provided by the National Research Foundation of Korea (NRF), funded by the Korean Government through the Ministry of Science and ICT (MSIT) (No. 2020R1A2C1102451 and 2023R1A2C1007243).

AUTHOR DISCLOSURE STATEMENT

The authors declare no conflict of interest.

AUTHOR CONTRIBUTIONS

Concept and design: HMK, KSK. Analysis and interpretation: HMK, Yerin K, Yuri K, KSK. Data collection: HMK, KSK. Writing the article: HMK, KSK. Critical revision of the article: YJK, KSK. Final approval of the article: all authors. Statistical analysis: HMK. Obtained funding: KSK. Overall responsibility: KSK.

REFERENCES

Akbari S, Arslan N, Senturk S, Erdal E. Next-generation liver medicine using organoid models. Front Cell Dev Biol. 2019. 7:345. https://doi.org/10.3389/fcell.2019.00345

Bak MJ, Truong VL, Ko SY, Nguyen XN, Ingkasupart P, Jun M, et al. Antioxidant and hepatoprotective effects of procyanidins from wild grape (*Vitis amurensis*) seeds in ethanol-induced cells and rats. Int J Mol Sci. 2016. 17:758. https://doi.org/10.3390/ijms17050758

Bell CC, Hendriks DF, Moro SM, Ellis E, Walsh J, Renblom A, et al. Characterization of primary human hepatocyte spheroids as a model system for drug-induced liver injury, liver function and disease. Sci Rep. 2016. 6:25187. https://doi.org/10.1038/srep25187

Beppu F, Hosokawa M, Niwano Y, Miyashita K. Effects of dietary fucoxanthin on cholesterol metabolism in diabetic/obese KK-A(y) mice. Lipids Health Dis. 2012. 11:112. https://doi.org/10.1186/1476-511x-11-112

Brooks A, Liang X, Zhang Y, Zhao CX, Roberts MS, Wang H, et al. Liver organoid as a 3D *in vitro* model for drug validation and toxicity assessment. Pharmacol Res. 2021. 169:105608. https://doi.org/10.1016/j.phrs.2021.105608

Builes-Montaño CE, Lema-Perez L, Garcia-Tirado J, Alvarez H. Main glucose hepatic fluxes in healthy subjects predicted from a phenomenological-based model. Comput Biol Med. 2022. 142:105232. https://doi.org/10.1016/j.compbiomed.2022.105232

Carvalho JR, Verdelho Machado M. New insights about albumin and liver disease. Ann Hepatol. 2018. 17:547-560.

Charni-Natan M, Goldstein I. Protocol for primary mouse hepatocyte isolation. STAR Protoc. 2020. 1:100086. https://doi.org/

10.1016/j.xpro.2020.100086
Chen X, Ding Y, Song J, Kan J. Hypolipidaemic effect and mechanism of paprika seed oil on Sprague-Dawley rats. J Sci Food Agric. 2017. 97:4242-4249.
Chu Q, Gu X, Zheng Q, Zhu H. Regulatory mechanism of HIF-1α and its role in liver diseases: a narrative review. Ann Transl Med. 2022. 10:109. https://doi.org/10.21037/atm-21-4222
Clemens DL. Use of cultured cells to study alcohol metabolism. Alcohol Res Health. 2006. 29:291-295.
EFSA Scientific Committee. Guidance on conducting repeated-dose 90-day oral toxicity study in rodents on whole food/feed. EFSA J. 2011. 9:2438. https://doi.org/10.2903/j.efsa.2011.2438
Gómez-Mariano G, Matamala N, Martínez S, Justo I, Marcacuzco A, Jimenez C, et al. Liver organoids reproduce alpha-1 antitrypsin deficiency-related liver disease. Hepatol Int. 2020. 14:127-137.
Han HS, Kang G, Kim JS, Choi BH, Koo SH. Regulation of glucose metabolism from a liver-centric perspective. Exp Mol Med. 2016. 48:e218. https://doi.org/10.1038/emm.2015.122
Harrison SP, Baumgarten SF, Verma R, Lunov O, Dejneka A, Sullivan GJ. Liver organoids: recent developments, limitations and potential. Front Med. 2021. 8:574047. https://doi.org/10.3389/fmed.2021.574047
Horton JD, Goldstein JL, Brown MS. SREBPs: activators of the complete program of cholesterol and fatty acid synthesis in the liver. J Clin Invest. 2002. 109:1125-1131.
Hu H, Gehart H, Artegiani B, LÖpez-Iglesias C, Dekkers F, Basak O, et al. Long-term expansion of functional mouse and human hepatocytes as 3D organoids. Cell. 2018. 175:1591-1606.e19.
Huch M, Koo BK. Modeling mouse and human development using organoid cultures. Development. 2015. 142:3113-3125.
Jonsson M, Jestoi M, Nathanail AV, Kokkonen UM, Anttila M, Koivisto P, et al. Application of OECD guideline 423 in assessing the acute oral toxicity of moniliformin. Food Chem Toxicol. 2013. 53:27-32.
Jungermann K, Kietzmann T. Zonation of parenchymal and nonparenchymal metabolism in liver. Annu Rev Nutr. 1996. 16:179-203.
Katz GG, Shear NH, Malkiewicz IM, Valentino K, Neuman MG. Signaling for ethanol-induced apoptosis and repair *in vitro*. Clin Biochem. 2001. 34:219-227.
Kim J, Koo BK, Knoblich JA. Human organoids: model systems for human biology and medicine. Nat Rev Mol Cell Biol. 2020a. 21:571-584.
Kim S, Yoon Y, Oh S. Suggestion of a safety evaluation procedure to improve probiotic safety. J Dairy Sci Biotechnol. 2020b. 38:99-111.
Kratochvil MJ, Seymour AJ, Li TL, Paşca SP, Kuo CJ, Heilshorn SC. Engineered materials for organoid systems. Nat Rev Mater. 2019. 4:606-622.
Lancaster MA, Knoblich JA. Organogenesis in a dish: modeling development and disease using organoid technologies. Science. 2014. 345:1247125. https://doi.org/10.1126/science.1247125
Lee HY. Approval of functional ingredient of health/functional foods in Korea. Food Ind Nutr. 2013. 18:1-7.
Liao CJ, Huang PS, Chien HT, Lin TK, Yeh CT, Lin KH. Effects of thyroid hormones on lipid metabolism pathologies in non-alcoholic fatty liver disease. Biomedicines. 2022. 10:1232. https://doi.org/10.3390/biomedicines10061232
Liu S, Hou W, Yao P, Zhang B, Sun S, Nüssler AK, et al. Quercetin protects against ethanol-induced oxidative damage in rat primary hepatocytes. Toxicol In Vitro. 2010. 24:516-522.
Liu S, Wu Z, Guo S, Meng X, Chang X. Polyphenol-rich extract from wild *Lonicera caerulea* berry reduces cholesterol accumulation by mediating the expression of hepatic miR-33 and miR-122, HMGCR, and CYP7A1 in rats. J Funct Foods. 2018. 40:648-658.
Liu S, Yeh TH, Singh VP, Shiva S, Krauland L, Li H, et al. β-Catenin is essential for ethanol metabolism and protection against alcohol-mediated liver steatosis in mice. Hepatology. 2012. 55:931-940.
Livak KJ, Schmittgen TD. Analysis of relative gene expression data using real-time quantitative PCR and the $2^{-\Delta\Delta C_T}$ method. Methods. 2001. 25:402-408.
Matson L, Liangpunsakul S, Crabb D, Buckingham A, Ross RA, Halcomb M, et al. Chronic free-choice drinking in crossed high alcohol preferring mice leads to sustained blood ethanol levels and metabolic tolerance without evidence of liver damage. Alcohol Clin Exp Res. 2013. 37:194-201.
Milani-Nejad N, Janssen PM. Small and large animal models in cardiac contraction research: advantages and disadvantages. Pharmacol Ther. 2014. 141:235-249.
Miller A, Jedrzejczak WW. Albumin--biological functions and clinical significance. Postepy Hig Med Dosw. 2001. 55:17-36.
MFDS (Ministry of Food and Drug Safety). Toxicity test method guidelines for food, etc.—acute oral toxicity. 2021a [cited 2021 Sep 30]. Available from: https://www.mfds.go.kr/brd/m_1060/view.do?seq=14916&srchFr=&srchTo=&srchWord=&srchTp=&itm_seq_1=0&itm_seq_2=0&multi_itm_seq=0&company_cd=&company_nm=&page=1
MFDS (Ministry of Food and Drug Safety). Toxicity test method guidelines for food, etc. 2021b [cited 2021 Sep 30]. Available from: https://www.mfds.go.kr/brd/m_1060/view.do?seq=14917
Miyajima A, Tanaka M, Itoh T. Stem/progenitor cells in liver development, homeostasis, regeneration, and reprogramming. Cell Stem Cell. 2014. 14:561-574.
Nakamura T, Sato T. Advancing intestinal organoid technology toward regenerative medicine. Cell Mol Gastroenterol Hepatol. 2017. 5:51-60.
National Institute on Alcohol Abuse and Alcoholism (NIAAA). Alcohol metabolism: An update. NIAAA. 2007. p 1-6.
Nuciforo S, Heim MH. Organoids to model liver disease. JHEP Rep. 2020. 3:100198. https://doi.org/10.1016/j.jhepr.2020.100198
Organisation for Economic Co-operation and Development (OECD). OECD guideline for testing of chemicals: test no. acute oral toxicity—acute toxic class method. OECD. 2001.
Peng WC, Kraaier LJ, Kluiver TA. Hepatocyte organoids and cell transplantation: What the future holds. Exp Mol Med. 2021. 53:1512-1528.
Qu M, Xiong L, Lyu Y, Zhang X, Shen J, Guan J, et al. Establishment of intestinal organoid cultures modeling injury-associated epithelial regeneration. Cell Res. 2021. 31:259-271.
Radko L, Śniegocki T, Sell B, Posyniak A. Metabolomic profile of primary turkey and rat hepatocytes and two cell lines after chloramphenicol exposure. Animals. 2019. 10:30. https://doi.org/10.3390/ani10010030
Rezakhani S, Gjorevski N, Lutolf MP. Extracellular matrix requirements for gastrointestinal organoid cultures. Biomaterials. 2021. 276:121020. https://doi.org/10.1016/j.biomaterials.2021.121020
Rizki-Safitri A, Shinohara M, Miura Y, Danoy M, Tanaka M, Miyajima A, et al. Efficient functional cyst formation of biliary epithelial cells using microwells for potential bile duct organisation *in vitro*. Sci Rep. 2018. 8:11086. https://doi.org/10.1038/s41598-018-29464-w
Rose S, Ezan F, Cuvellier M, Bruyère A, Legagneux V, Langouët S, et al. Generation of proliferating human adult hepatocytes using optimized 3D culture conditions. Sci Rep. 2021. 11:515. https://doi.org/10.1038/s41598-020-80019-4
Sendi H, Mead I, Wan M, Mehrab-Mohseni M, Koch K, Atala A, et al. miR-122 inhibition in a human liver organoid model leads

to liver inflammation, necrosis, steatofibrosis and dysregulated insulin signaling. PLoS One. 2018. 13:e0200847. https://doi.org/10.1371/journal.pone.0200847

Shulman M, Nahmias Y. Long-term culture and coculture of primary rat and human hepatocytes. In: Randell SH, Fulcher ML, editors. Epithelial Cell Culture Protocols. 2nd ed. Springer. 2012. p 287-302.

Trapani L, Segatto M, Pallottini V. Regulation and deregulation of cholesterol homeostasis: The liver as a metabolic "power station". World J Hepatol. 2012. 4:184-190.

Zakhari S. Overview: how is alcohol metabolized by the body? Alcohol Res Health. 2006. 29:245-254.

Zhu D, Rostami MR, Zuo WL, Leopold PL, Crystal RG. Single-cell transcriptome analysis of mouse liver cell-specific tropism and transcriptional dysregulation following intravenous administration of AAVrh.10 vectors. Hum Gene Ther. 2020. 31:590-604.